A Hierarchically Coordinated Operation and Control Scheme for DC Microgrid Clusters under Uncertainty

Xu, Qianwen; Xu, Yan; Xu, Zhao Z.; Xie, Lihua Xie; Blaabjerg, Frede

Published in:
I E E E Transactions on Sustainable Energy

DOI (link to publication from Publisher):
10.1109/TSTE.2020.2991096

Publication date:
2021

Document Version
Accepted author manuscript, peer reviewed version

A Hierarchically Coordinated Operation and Control Scheme for DC Microgrid Clusters under Uncertainty

Qianwen Xu, *Member, IEEE,* Yan Xu, *Senior Member, IEEE,* Zhao Xu, *Senior Member, IEEE,* Lihua Xie, *Fellow, IEEE,* and Frede Blaabjerg, *Fellow, IEEE*

***Abstract*—In the existing works of microgrid clusters, operation and real-time control are normally designed separately in a hierarchical architecture, with the real-time control in the primary and secondary levels, and operation in the tertiary level. This paper proposes a hierarchically coordinated control scheme for DC MG clusters under uncertainty. In each MG, the tertiary level controller optimizes the operating cost in the MG by taking into account the real-time uncertainties of renewable generations and loads deviated from the forecasting data; and the primary controller responds to the real-time power fluctuations through an optimised droop curve. The hierarchically coordinated optimization problem is formulated to optimize the power set points and droop curve coefficients simultaneously under uncertainties using an adjustable robust optimization model. For the MG cluster, the energy sharing of each MG in the cluster is optimized to minimize the total operating cost and the transmission loss. The overall optimization problem is solved in a distributed manner by alternating direction method of multipliers (ADMM) where each MG entity only exchanges boundary information (i.e. the power exchange of MG entity with the MG cluster), thus information privacy and plug-and-play feature of each MG are guaranteed. The proposed approach optimally coordinates the operation and real-time control layers of a DC MG cluster with uncertainties; it achieves decentralized power sharing at the real-time control layer and distributed optimization at the operation layer, featuring high scalability, reliability and economy. Case studies of a DC MG cluster are conducted in Matlab/Simulink in order to demonstrate the effectiveness of the proposed approach.**

***Index Terms*—DC microgrid cluster, coordination, operation, real-time control, distributed optimization**

I. Introduction

MICROGRIDS (MGs), which integrate distributed resources, energy storage systems and local loads, provide promising solutions for the integration of renewable energy sources into grids [1]. Extensive research works have been conducted for AC MGs due to their compatibility to the existing power grids [2], [3]. In recent years, DC MGs are gaining increasing attention as they provide efficient interfaces for integrating a large number of distributed energy sources (e.g. solar PV, fuel cell and energy storage units) and loads (e.g. LED, electronics, motor drives, electric vehicle chargers), which are DC by nature [4], [5]. Also DC MGs do not suffer from issues such as synchronization, harmonics, etc., compared with their AC counterparts.

Multiple DC MGs can be connected with each other and form a DC MG cluster, or a community [6], [7], to enhance the overall system resiliency, efficiency and economy. The hierarchical control scheme has been widely adopted as a standardized solution for the control and management of DC MGs and MG clusters, which comprises of primary, secondary and tertiary control levels that act on different time scales: the primary and secondary levels deal with the real-time control issues (e.g. power management and voltage regulation in seconds) and the tertiary level deals with the operation issues (i.e. economic dispatch and energy scheduling in minutes and hours) [4], [5], [8], [9]. However, existing works only study the real-time control issues or only investigate the operation issues. There is no mutual coordination in the real-time control and long term operation layer.

There are many works about real-time control and power management of DC MGs [4], [5], [9], [10]. In these works, they track the power/voltage variables at the reference values, and droop control is employed to achieve proportional power sharing with the real-time power balance; the economic issue is usually ignored. Ref [11] proposes a cost-prioritized droop scheme for autonomous power sharing with reduced operational cost. Ref [12] proposes an incremental cost based droop control approach for decentralized economic power sharing without communication links. A multi-objective adaptive control framework is proposed for battery management in DC MGs [13]. Ref [14] proposes a distributed control method to achieve economic power management and voltage regulation. However, these approaches are for real-time power management and they do not consider the electricity price as well as the state-of-charge management of energy storage systems in the long term, thus the optimal operation is not achieved.

There are many works on energy management of MG clusters. A two-level hierarchical optimization method is proposed in [15] for energy management of a MG community; the lower

This work was supported in part by Ministry of Education (MOE), Republic of Singapore, under grant AcRF TIER 1 2019-T1-001-069 (RG75/19), in part by National Research Foundation (NRF) of Singapore under project NRF2018-SR2001-018, and in part by Wallenberg-NTU Presidential Postdoc Fellowship in Nanyang Technological University, Singapore. Y. Xu's work is supported by Nanyang Assistant Professorship from Nanyang Technological University, Singapore.

Q. Xu, Y. Xu and L. Xie are with the school of Electrical and Electronic Engineering, Nanyang Technological University, Singapore, e-mail:qianwen.xu@ntu.edu.sg, xuyan@ntu.edu.sg,elhxie@ntu.edu.sg

Z. Xu is with the Department of Electrical Engineering, The Hong Kong Polytechnic University, Kowloon, Hong Kong, and is also with School of Electrical and Information Engineering, Changsha University of Science and Technology, Changsha 410114, China, e-mail: eezhaoxu@polyu.edu.hk.

F. Blaabjerg is with the Department of Energy Technology, Aalborg University, Denmark, e-mail: fbl@et.aau.dk

This article has been accepted for publication in a future issue of this journal, but has not been fully edited. Content may change prior to final publication. Citation information: DOI 10.1109/TSTE.2020.2991096, IEEE Transactions on Sustainable Energy

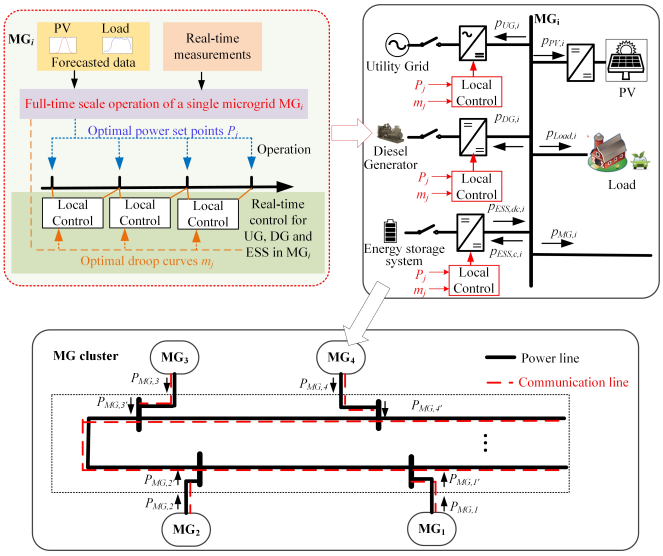

Fig. 1. The architecture of a DC MG cluster with the proposed coordinated control scheme

level optimizes the power output of individual MGs and the higher level determines the power exchanges among MGs; but the uncertainties are not considered. In [16], a resilient operation framework is proposed for a multi-microgrid system to achieve the optimal power flow, optimal load shedding and optimal topology reconfiguration while maintaining the frequency stability after islanding events; while the focus of [16] is on the emergency control, where the real-time source and load uncertainties are not considered. Ref [17] proposes a stochastic bi-level optimization strategy for networked MGs in a distribution system to minimize the total operation costs considering the uncertainties of DG output. A distributed adjustable robust optimal scheduling algorithm is proposed in [18] to optimize the total operational cost of multiple MGs in a real-time electricity market considering the uncertainties of renewable sources and loads. A bi-level learning based power management is proposed in [19] to achieve economic operation of networked MGs with incomplete information of MG models, where a cooperative agent optimizes the revenue of all MGs by setting the price signal with limited information at higher level, and each MG provides optimal scheduling individually to respond to the price signal at lower level. In [20], an intelligent energy management method is proposed to optimize the profit based on deep neural network (DNN) and model free reinforcement learning techniques; a distribution system operator (DSO) learns the multi-microgrid response using DNN without the user's information and DSO selects the pricing strategy from reinformence learning to optimize the decision. However, for all these works on energy management, they optimize the energy/power scheduling in the operation time scale, which is in several minutes or hours; and the real-time responses of local control units are not considered in the optimization process, which will deviate the scheduling variables due to real-time uncertainties. Moreover, all these works are for AC MG clusters.

Based on the above literature review, in most existing works, the dispatch decisions and real-time control settings are separately determined without the mutual coordination; as a result, the real-time control variables may deviate from the scheduling set points during a scheduling time interval due to the uncertainties of renewable generations and loads. To address this issue, this paper deals with full-time scale coordinated operation and control of DC MG clusters. In each MG, the scheduling power set points and optimal droop curves are simultaneously optimized over a scheduling horizon to minimize the operating cost considering the primary controller's response to uncertainties of renewable generations and loads in real time; the primary controllers respond to the real-time power fluctuations through the optimal droop curves near the optimal power set points. The hierarchically coordinated optimization problem is formulated as an affinely adjustable robust optimization model. For the MG cluster, energy sharing of each MG is optimized to minimize the overall operating cost and transmission loss in a distributed manner by ADMM that each MG makes individual decisions and only needs to exchange boundary information with each other (i.e. the power exchange of each MG entity with the cluster) to guarantee the information privacy of each entity and the plug-and-play feature. The contributions of this paper are summarized as follows

1) The proposed approach optimally coordinates the operation and real-time control to minimize the total operating cost with the guaranteed real-time power balance.

2) With the robust and distributed optimization for the DC MG cluster, uncertainties are managed locally within each MG, and the information privacy of each MG entity is preserved.

3) The proposed approach achieves decentralized power sharing at the real-time control layer and distributed optimization at the operation layer, thus it features high scalability and reliability, especially for a MG cluster with open-boundary and plug-and-play characteristics.

The rest of the paper is organized as follows: Section II describes the architecture of the DC MG cluster and the proposed coordination scheme. Section III formulates the optimization problem for a single MG with the proposed coordinated operation and control scheme. Section IV illustrates the distributed optimization solution of the MG cluster system. Case studies are performed for verification in Section V. Conclusions are drawn in Section VI.

II. DC MG CLUSTER AND PROPOSED HIERARCHICALLY COORDINATED OPTIMIZATION MODEL

Fig. 1 presents the physical structure of a DC MG cluster with the proposed hierarchically coordinated operation and control scheme. An individual DC MG consists of various sources such as renewable energy sources (RESs, e.g. PV), dispatchable distributed generators (DGs, e.g. fuel cells and diesel generators) and energy storage systems (ESSs). It can either be connected to the utility grid (UG) or isolated. The DC MG cluster is formed by interconnecting individual DC MGs through a DC network.

Generally, the objective of the MG cluster operation is to maximize the utilization of RESs and minimize the operational cost by scheduling the energy output of UG, DGs and

This article has been accepted for publication in a future issue of this journal, but has not been fully edited. Content may change prior to final publication. Citation information: DOI 10.1109/TSTE.2020.2991096, IEEE Transactions on Sustainable Energy

ESSs, and energy exchange among MGs, while satisfying the operational constraints such as the power balance constraints, power and energy capacity limitations and transmission capacity limitation. The scheduling time interval is normally at several minutes to hours. However, the responses of RESs and power electronics converters are in milliseconds to seconds. Although the forecasted outputs of RESs and load can be in a reasonably accurate range, they may still vary randomly from the predictions. Once the uncertain power outputs deviate from the predicted values significantly within a scheduling interval, the economic optimality may be deteriorated and the operational constraints may be violated.

To optimize the overall operational cost of the DC MG cluster with uncertainties and to ensure system stable and economic operation in real time, a hierarchically coordinated control scheme is proposed in this paper, where the power setpoints and droop curves are simultaneously optimized, as illustrated in Fig. 1. In the operation layer, each MG optimizes the scheduling power set points and optimal droop curves over a scheduling horizon to minimize the operating cost with the consideration of the real-time controller's response to uncertainties in real time. In the real-time control layer, the real-time droop controllers respond to the real-time power fluctuations through the optimal droop curves near the optimal power set points.

For the overall coordination of the MG cluster, an optimization model is formulated to optimize the total operational costs and transmission loss, and ADMM algorithm is applied for distributed operation: each MG optimizes its own operational cost to get optimal droop curves; in the meantime, each MG only exchanges boundary information (i.e. the power exchange information of each MG in the cluster, as illustrated in Fig. 1), so that the total power loss of the network system is minimized. This also guarantees the information privacy of each MG and the plug-and-play scalability.

III. The Coordinated Optimization Model for a Single Microgrid

This section considers the coordinated operation and control of a single MG. First, the optimization model for the total operational cost is presented. Then the real-time control problem under uncertainty is described. Finally, a hierarchically coordinated model is proposed to optimize the scheduling power set points and droop curves simultaneously considering the real-time uncertainties.

A. Operation model

1) Objective function: The objective for MG i is to minimize the total operating cost including UG, DGs and ESSs within the time horizon $\mathcal{T}$. Thus the objective function is given by

$$\min_{\mathbf{p}_i(t)\forall t\in\mathcal{T}} \sum_{t\in\mathcal{T}} f(\mathbf{p}_i(t)) = \sum_{t\in\mathcal{T}} [C_{\mathrm{UG},i}(t) + C_{\mathrm{DG},i}(t) + C_{\mathrm{ESS},i}(t)] \tag{1}$$

where $C_{\mathrm{UG},i}(t)$, $C_{\mathrm{DG},i}(t)$ and $C_{\mathrm{ESS},i}(t)$ are cost functions of UG, DGs and ESSs. $\mathbf{p}_i(t) := \{p_{\mathrm{UG},i}(t), p_{\mathrm{DG},i}(t), p_{\mathrm{ESS,c},i}(t), p_{\mathrm{ESS,dc},i}(t), p_{\mathrm{MG},i}(t)\}$, $t \in \mathcal{T}$ are decision variables; $p_{\mathrm{UG},i}(t)$, $p_{\mathrm{DG},i}(t)$, $p_{\mathrm{ESS,c},i}(t)$, $p_{\mathrm{ESS,dc},i}(t)$ and $p_{\mathrm{MG},i}(t)$ represent real power output of UG, DG, ESS (charge and discharge) and power exchange between the i-th MG and the network during time slot *t*, respectively.

The cost function of UG is described by

$$C_{\mathrm{UG},i}(t) = \lambda(t) p_{\mathrm{UG},i}(t) \tag{2}$$

where $\lambda(t)$ is the electricity price during time slot *t*.

For dispatchable DGs like diesel generator and fuel cell, the widely used quadratic cost function is adopted [11], expressed as

$$C_{\mathrm{DG},i}(t) = a_{DGi} p^2_{\mathrm{DG},i}(t) + b_{DGi} p_{\mathrm{DG},i}(t) + c_{DGi} \tag{3}$$

where a_{DGi}, b_{DGi} and c_{DGi} are constants.

The cost function of ESS is obtained as [21]:

$$C_{\mathrm{ESS},i}(t) = c_{\mathrm{ESS},i}(p_{\mathrm{ESS,dc},i}(t) + p_{\mathrm{ESS,c},i}(t)) \tag{4}$$

where c_{ESSi} is a constant coefficient.

2) Constraints: The operation constraints including the power balance constraint and the power/energy limitation constraints are:

$$\begin{aligned} &p_{\mathrm{UG},i}(t) + p_{\mathrm{DG},i}(t) + p_{\mathrm{ESS,dc},i}(t) - p_{\mathrm{ESS,c},i}(t) \\ &-p_{\mathrm{MG},i}(t) = p_{Load,i}(t) - p_{\mathrm{PV},i}(t), \forall t \in \mathcal{T} \end{aligned} \tag{5}$$

$$0 \le p_{\mathrm{UG},i}(t) \le P_{\mathrm{UG,max},i}, \forall t \in \mathcal{T} \tag{6}$$

$$P_{\mathrm{DG,min},i} \le p_{\mathrm{DG},i}(t) \le P_{\mathrm{DG,max},i}, \forall t \in \mathcal{T} \tag{7}$$

$$\begin{aligned} -R_{\mathrm{DG,down},i} \le p_{\mathrm{DG},i}(t) - p_{\mathrm{DG},i}(t-\Delta t) \\ \le R_{\mathrm{DG,up},i}, \forall t \in \mathcal{T} \end{aligned} \tag{8}$$

$$0 \le p_{\mathrm{ESS,dc},i}(t) \le P_{\mathrm{ESS,dc,max},i}, \forall t \in \mathcal{T} \tag{9}$$

$$0 \le p_{\mathrm{ESS,c},i}(t) \le P_{\mathrm{ESS,c,max},i}, \forall t \in \mathcal{T} \tag{10}$$

$$\begin{aligned} E_{\mathrm{ESS},i}(t) = E_{\mathrm{ESS},i}(t-\Delta t) + p_{\mathrm{ESS,c},i}(t)\eta_{\mathrm{ESS,c},i}\Delta t - \\ \frac{p_{\mathrm{ESS,dc},i}(t)\Delta t}{\eta_{\mathrm{ESS,dc},i}}, \forall t \in \mathcal{T} \end{aligned} \tag{11}$$

$$E_{\mathrm{ESS,min},i} \le E_{\mathrm{ESS},i}(t) \le E_{\mathrm{ESS,max},i}, \forall t \in \mathcal{T} \tag{12}$$

$$p_{\mathrm{ESS,dc},i}(t) p_{\mathrm{ESS,c},i}(t) = 0, \forall t \in \mathcal{T} \tag{13}$$

where Eq. (5) represents the power balance constraint within MG i; Eq. (6) describes the power exchange limitation of MG i with the UG. Eqs. (7) and (8) illustrate the power capacity and ramp rate constraints of DG. The charging and discharging rate limitations of ESS are expressed in Eq. (9) and Eq. (10), respectively. The energy status balance and constraints of ESS are given by Eq. (11) and Eq. (12), respectively, where $E_{\mathrm{ESS,min},i}$ denotes energy status, $\eta_{\mathrm{ESS,dc},i}$ and $\eta_{\mathrm{ESS,c},i}$ denote the discharging and charging efficiencies. The complementary characteristics of charging and discharging power of ESS is depicted by Eq. (13). Constraint (13) can be removed by following similar procedure of the proof in appendix in [22].

The operation model of MG i is obtained by combining Eq. (1) with constraints (5)-(12). If the forecasting values of PV and load are perfect and equal to $P_{\mathrm{PV},i}(t)$ and $P_{Load,i}(t)$, the optimal power setpoints $\mathbf{p}_i(t)$ can be obtained as

This article has been accepted for publication in a future issue of this journal, but has not been fully edited. Content may change prior to final publication. Citation information: DOI 10.1109/TSTE.2020.2991096, IEEE Transactions on Sustainable Energy

$P_{\text{UG},i}(t), P_{\text{DG},i}(t), P_{\text{ESS,c},i}(t), P_{\text{ESS,dc},i}(t)$ and $P_{\text{MG},i}(t)$. However, as mentioned previously, though the forecasted outputs of PV and load can be in a reasonably accurate range, they still vary randomly from the expected values. Thus the uncertainties during a scheduling interval should be considered.

B. Real-time control model

For the implementation of real-time control for MG i, PV operates at MPPT mode; UG, DG and ESS operate in droop control mode to respond to the transient power fluctuations caused by PV and load [23], as illustrated in Fig. 1.

The classic droop controller for a DC MG is expressed as

$$v_j = V_j - m_j(p_j - P_j) \tag{14}$$

where v_j and p_j are real-time output voltage and power of jth DG; V_j and P_j are the reference values of output voltage and power of jth DG; the droop coefficient m_j is determined by the maximum voltage deviation $\Delta V_{\max}$ and power rating of jth DG $P_{j,\max}$:

$$m_j = \frac{\Delta V_{\max}}{P_{j,\max}} \tag{15}$$

But classic droop controller based on eq. (15) does not consider economic issue and operation constraints. In this paper, the response of the droop controllers to real-time uncertainties will be modeled in the overall optimization problem to get the optimal droop curves for real-time controllers.

For different components, their droop curves are given by

$$v_i - V_i = m_{UG,i}(p_{UG,i} - P_{UG,i}) \tag{16}$$

$$v_i - V_i = m_{DG,i}(p_{DG,i} - P_{FC,i}) \tag{17}$$

$$v_i - V_i = m_{ESS,i}(p_{ESS,i} - P_{ESS,i}) \tag{18}$$

where V_i is the reference voltage value; $P_{UG,i}$, $P_{DG,i}$ and $P_{ESS,i}$ are optimal power set points; $m_{UG,i}$, $m_{DG,i}$ and $m_{ESS,i}$ are optimal droop coefficients. They will be optimized and updated from the operation layer in MG i.

The variations of real-time values of PV and load to their forecasting values are denoted as $\xi_{\text{PV},i}(t)$, they can be depicted by zero-mean uncertainty intervals, given by

$$p_{\text{PV},i}(t) - P_{\text{PV},i}(t) = \xi_{\text{PV},i}(t) \in \quad [-\xi^{\max}_{\text{PV},i}, \xi^{\max}_{\text{PV},i}] \tag{19}$$

$$p_{\text{Load},i}(t) - P_{\text{Load},i}(t) = \xi_{\text{Load},i}(t) \in \quad [-\xi^{\max}_{\text{Load},i}, \xi^{\max}_{\text{Load},i}] \tag{20}$$

The interval range of the PV generation and load demand are obtained from interval forecasting techniques [24], which provide expected values and variation ranges. The bounds of the predicted uncertainty variation range are set as the lower and upper bounds in the uncertainty set.

Then the aggregated uncertainties are obtained as

$$\xi_i = \xi_{\text{Load},i} - \xi_{\text{PV},i} \in [-\xi^{\max}_i, \xi^{\max}_i] \tag{21}$$

where the boundary of the aggregated uncertainty is given by $\xi^{\max}_i = \xi^{\max}_{\text{Load},i} + \xi^{\max}_{\text{PV},i}$.

Based on the adjustable robust optimization approach [29], the real-time power sharing of UG, DG and ESS in relation to their uncertainties is respectively given by

$$p_{\text{UG},i} - P_{\text{UG},i} = \beta_{\text{UG},i}\xi_i \tag{22}$$

$$p_{\text{DG},i} - P_{\text{DG},i} = \beta_{\text{DG},i}\xi_i \tag{23}$$

$$p_{\text{ESS},i} - P_{\text{ESS,dc},i} + P_{\text{ESS,c},i} = \beta_{\text{ESS},i}\xi_i \tag{24}$$

$$\beta_{\text{UG},i} + \beta_{\text{DG},i} + \beta_{\text{ESS},i} = 1 \tag{25}$$

where $\beta_{\text{UG},i}$, $\beta_{\text{DG},i}$ and $\beta_{\text{ESS},i}$ are the participation factors of UG, DG and ESS in sharing the uncertain power variation from the the load and PV. The relationship between participation factors and droop coefficients is obtained as

$$m_{UG,i} = \frac{k_i}{\beta_{UG,i}}, m_{UG,i} \in \left(0, \frac{\Delta V_{\max}}{P_{UG,\max}}\right) \tag{26}$$

$$m_{DG,i} = \frac{k_i}{\beta_{DG,i}}, m_{DG,i} \in \left(0, \frac{\Delta V_{\max}}{P_{DG,\max}}\right) \tag{27}$$

$$m_{ESS,i} = \frac{k_i}{\beta_{ESS,i}}, m_{ESS,i} \in \left(0, \frac{\Delta V_{\max}}{P_{ESS,\max}}\right) \tag{28}$$

with

$$k_i = \min\left\{\frac{\beta_{UG,i}\Delta V_{\max}}{P_{UG,\max}}, \frac{\beta_{DG,i}\Delta V_{\max}}{P_{DG,\max}}, \frac{\beta_{ESS,i}\Delta V_{\max}}{P_{ESS,\max}}\right\} \tag{29}$$

It should be noted that in some cases, some of the participation factors are too small which means the corresponding sources do not participate in sharing the uncertain fluctuations. This may lead to a very small value of k_i according to (29). To avoid this situation, the participation factor less than 0.1 will be seen as not taking part in uncertain power sharing and the corresponding droop coefficient will be set at a relatively large value, which is 10 in this paper.

C. Hierarchical coordination

Combination of the operation model in (1)-(12) with the real-time control model in (19)-(27), the coordinated model is formulated as an adjustable robust optimization model [25], given by

$$\begin{aligned}&\min_{\mathbf{P}_i(t),\beta_i(t),\forall t\in\mathcal{T}} \mathbb{E}\sum_{t\in\mathcal{T}} f(\mathbf{P}_i(t),\beta_i(t)) = \\ &\sum_{t\in\mathcal{T}}[C_{\text{UG},i}(t) + C_{\text{DG},i}(t) + C_{\text{ESS},i}(t)] \\ &\text{s.t.} \\ &\text{reformulated } (5)-(12) \text{ with base-point values } \mathbf{P}_i(t) \\ &\text{(A.7)-(A.11) in Appendix}\end{aligned} \tag{30}$$

where power set point values $\mathbf{P}_i(t) := \{P_{\text{UG},i}(t), P_{\text{DG},i}(t), P_{\text{ESS,c},i}(t), P_{\text{ESS,dc},i}(t), P_{\text{MG},i}(t)\}$, $t \in \mathcal{T}$ and participation factors $\beta_i(t) := \{\beta_{\text{UG},i}(t), \beta_{\text{DG},i}(t), \beta_{\text{ESS},i}(t)\}, t \in \mathcal{T}$ are decision variables. The droop coefficients are obtained by (26)-(29) based on participation factors. Reformulated constraints (5)-(12) are obtained by substituting the power set point values $\mathbf{P}_i(t)$ for real-time values $\mathbf{p}_i(t)$ in (5)-(12). Robust counterparts of (5)-(12) are formulated by considering the real-time uncertainties in (21) and affinely droop curves in (22)-(25), which are presented in (A.7)-(A.11) in Appendix in detail.

It should also be mentioned that each MG can be integrated with multiple DGs and ESSs, with the additional DGs duplicating the variables related to subscript DG as DG, $DG2$, ...,

DGn and additional ESSs duplicating the variables related to subscript ESS as $ESS2$, ...,$ESSn$.

Remarks: We use the robust optimization method rather than a probabilistic method because of the following reasons [26], [27]: 1) a probabilistic method requires a probabilistic distribution function for the uncertainties, which is difficult to obtain in practice; 2) a probabilistic method requires scenario-based data to model uncertainties, which causes high computation burden; 3) a probabilistic method can only ensure the constraints probabilistically, not all the time. On the other hand, for robust optimization, it does not require the knowledge of probabilistic distribution function, it utilizes uncertainty sets to model uncertainties instead of a large number of scenarios and it can achieve a robust solution against the worst case so that all the constraints are satisfied. Though the robust optimization may lead to more conservative results as compared to the probabilistic approach, considering its advantages, robust optimization is selected in this work.

IV. Distributed optimization among MGs in a cluster

In the previous section, a coordinated control and optimization model for a single MG is developed to optimize the scheduling power set points and optimal droop curves with the consideration of the primary controller's response against uncertainties in real time. Based on the single MG model, this section develops an overall optimization model by interconnecting multiple MGs through a network.

A. The overall optimization model for the MG cluster

The DC MG cluster is formed by interconnecting multiple MGs through a DC network. Based on the branch power flow model in [28], the DC network model is depicted as

$$\sum_{k:k\to j} P_{jk}(t) = \sum_{i:i\to j} (P_{ij}(t) - r_{ij} l_{ij}(t)) + p_{\text{MG},j}(t), \quad \forall j \in \mathcal{N}, t \in \mathcal{T} \tag{31}$$

$$v_j(t) - v_k(t) = 2r_{jk}P_{jk}(t) - r_{jk}^2 l_{jk}(t), \forall j \to k \in \mathcal{E}, t \in \mathcal{T} \tag{32}$$

$$v_j(t) l_{jk}(t) = P_{jk}^2(t), \forall j \to k \in \mathcal{E}, t \in \mathcal{T} \tag{33}$$

where the DC network is denoted by a connected network $\mathcal{G}$:=$(\mathcal{N}, \mathcal{E})$, in which $\mathcal{N}$ is the set of buses connected with MGs and $\mathcal{E}$ is the set of transmission lines connecting the MGs. $l_{jk}(t) := I_{jk}^2(t)$, $v_j(t) := V_j^2(t)$, $P_{jk}(t)$, r_{jk} and $I_{jk}(t)$ are the power, resistor and current on line $j \to k$, $V_j(t)$ is the voltage magnitude of bus j.

The energy sharing information among interconnected MGs is optimized to minimize the total operating cost considering transmission loss. The overall optimization model is the summation of cost functions of all interconnected MGs and the transmission loss, expressed as

$$\begin{aligned} &\min_{\substack{\mathbf{P}_j(t),\beta_j(t),\\ P_{jk}(t),l_{jk}(t),v_j(t)\\ \forall j\in\mathcal{N}, j\to k\in\mathcal{E}, t\in\mathcal{T}}} \mathbb{E}\sum_{t\in\mathcal{T}}\{f(\mathbf{P}_i(t),\beta_i(t)) + \sum_{j:j\to k} l_{jk}(t) r_{jk}\} \\ &\text{reformulated } (5)-(12),(31)-(33),\text{(A.7)-(A.11)} \\ &v_{j,\min} \le v_j(t) \le v_{j,\max}, \forall j \in \mathcal{N}, t \in \mathcal{T} \\ &l_{jk}(t) \le l_{jk,\max}, \forall j \to k \in \mathcal{E}, t \in \mathcal{T} \end{aligned} \tag{34}$$

where the first term indicates the summation of cost functions of all interconnected MGs and the second term indicates the transmission loss on the DC network. $v_{j,\min}$ and $v_{j,\max}$ are the minimal and maximal limitations on the voltage magnitude of bus j. $l_{jk,\max}$ is the thermal current limitation on line $j \to k$.

B. Distributed optimization by ADMM

The optimization problem in (36) is a centralized optimization problem, which requires detailed models of each MG and may suffer from high computational burden if the system is large. To provide an efficient, scalable and information-privacy operation scheme, a distributed algorithm is developed using alternating direction method of multipliers (ADMM) [29]. Auxiliary variables, i.e., $P'_{\text{MG},i}(t), \forall i \in \mathcal{N}, t \in \mathcal{T}$, are introduced as duplications of $P_{\text{MG},i}(t), \forall i \in \mathcal{N}, t \in \mathcal{T}$. The auxiliary variables are optimized by the distribution operator, while the $P_{\text{MG},i}(t), \forall t \in \mathcal{T}$ is optimized by each MG. In addition, the auxiliary variables should meet the following condition, which is also denoted in Fig. 1:

$$P'_{\text{MG},i}(t) = P_{\text{MG},i}(t), \forall i \in \mathcal{N}, t \in \mathcal{T} \tag{35}$$

With the introduction of auxiliary variables and constraints (35), the optimization problem (34) can be solved distributedly by the standard ADMM [29] with the corresponding augmented Lagrangian formulated as

$$\begin{aligned} L_\rho(x,z,y) = \mathbb{E}\sum_{t\in\mathcal{T}} f(\mathbf{p}_i(t),\beta_i(t)) + \sum_{j:j\to k}\{l_{ij}(t)r_{ij} \\ + \sum_{i\in\mathcal{N}}[y_i(t)(P'_{\text{MG},i}(t) - P_{\text{MG},i}(t)) + \frac{\rho}{2}(P'_{\text{MG},i}(t) - P_{\text{MG},i}(t))^2]\} \end{aligned} \tag{36}$$

where x consists of decision variables (power set points $\mathbf{p}_i(t)$ and participation factors $\beta_i(t)$) in individual MGs including the anxiliary variable $P_{\text{MG},i}(t)$; z consists of decision variables $(P_{ij}(t), l_{ij}(t), v_j(t))$ in DC network and the anxiliary variable $P'_{\text{MG},i}(t)$.

Then the implementation of the ADMM for (36) is detailed as follows:

Initialization

The iteration time k is set at zero. The decision variables (power set point values and participation factors) in individual MGs are initialized at zero. The decision variables (power set point values) at the connection network are set at zero. Auxiliary variables $P'_{\text{MG},i}(t)$ and $P_{\text{MG},i}(t)$ are set at zero.

Step 1:

This article has been accepted for publication in a future issue of this journal, but has not been fully edited. Content may change prior to final publication. Citation information: DOI 10.1109/TSTE.2020.2991096, IEEE Transactions on Sustainable Energy

For MG i ($i \in \mathcal{N}$), it receives auxiliary variable $P^{',k}_{\text{MG},i}(t)$ from the DC network and updates its schedule by solving the optimization problem:

$$\begin{aligned}\mathbf{P}^{k+1}_{\text{MG},i} = &\underset{\mathbf{P}_i(t),\beta_i(t),\forall t\in\mathcal{T}}{\text{argmin}} \{\mathbb{E}\sum_{t\in\mathcal{T}} f(\mathbf{p}_i(t),\beta_i(t)) \\ &-y^k_i(t)P_{\text{MG},i}(t) + \frac{\rho}{2}(P_{\text{MG},i}(t) - P^{',k}_{\text{MG},i}(t))^2\} \\ &\text{s.t. reformulated}(5)-(12),(\text{A.7})\text{-}(\text{A.11})\end{aligned} \tag{37}$$

Step 2:

For the DC network, it receives auxiliary variable $P^{k+1}_{\text{MG},i}(t)$ from the MGs and update its schedule as

$$\begin{aligned}\mathbf{P}^{',k+1}_{\text{MG},i} = &\underset{P'_{\text{MG},i}(t),P_{ij}(t),l_{ij}(t),v_j(t)}{\text{argmin}} \sum_{t\in\mathcal{T}}\{l_{ij}(t)r_{ij} \\ &+\sum_{i\in\mathcal{N}}[y^k_i(t)P^{'}_{\text{MG},i}(t) + \frac{\rho}{2}(P^{'}_{\text{MG},i}(t) - P^{k+1}_{\text{MG},i}(t))^2]\} \\ &\text{s.t.}(31)-(33) \\ &v_{j,\min} \le v_j(t) \le v_{j,\max}, \forall j \in \mathcal{N}, t\in\mathcal{T} \\ &l_{ij}(t) \le l_{ij,\max}, \forall i\to j \in \mathcal{E}, t\in\mathcal{T}\end{aligned} \tag{38}$$

Convergence test

When the convergence condition $|\mathbf{P}^{',k+1}_{\text{MG},i} - \mathbf{P}^{k+1}_{\text{MG},i}|^2 \le tol$ is detected, the iterative process is completed and the results will be returned.

Otherwise, the iterative process will continue by updating $y^{k+1}_i(t) = y^k_i(t) + \rho(P^{',k+1}_{\text{MG},i}(t) - P^{k+1}_{\text{MG},i}(t))$ and $k = k+1$, and then go back to step 1.

Theorem 1 The convergence of the ADMM algorithm can be guaranteed to achieve optimal solution of the problem (34).

Proof: The subproblems in (37) and (38) are strictly convex. Based on the above implementation, there are two blocks in the ADMM with one for individual MGs in Step 1 and the other for the network in Step 2. According to the convergence proof in Appendix A of [29], the two block ADMM algorithm converge to achieve optimal solution.

V. Case Studies

A DC MG cluster with three interconnected DC MGs is tested in Matlab to verify the effectiveness of the proposed operation and control scheme in Figs. 1. MG1 is grid connected and has a DG, an ESS, a PV source and a lumped DC load. MG2 and MG3 both have two DGs, an ESS, a PV source and a lumped DC load. The three MGs are interconnected with each other with line impedance at 0.5008Ω and transmission line capacity at 100kW. The system parameters are listed in Table I. The time horizon is 24 hours and dispatch interval is 1 hour. The data of wholesale electricity price, PV profile and load demand are from [30]. The maximum forecast errors of PV $\xi^{\max}_{\text{PV},i}$ and load $\xi^{\max}_{\text{Load},i}$ are selected as 0.1 and 0.1 [31]. The equivalent load profiles ($P_{Load,i} - P_{PV,i}$) with uncertainties are shown in Fig. 2. The wholesale electricity price is shown in Fig. 3. Optimization problems are solved in Matlab at a desktop with an Intel i7-4770CPU@3.4GHz and 16GB RAM using Gurobi solver.

Fig. 4 shows the convergence curve of the total operational costs. It is shown that the value converges after 177 iterations and the optimal operational cost is achieved at $ 457. The time to calculate an update of the control variable is 25.5s for the system.

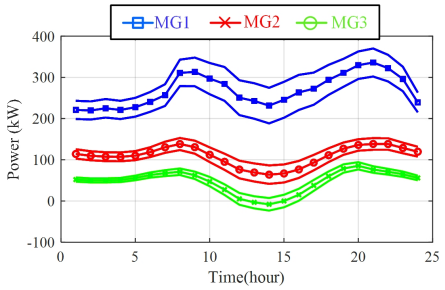

Fig. 2. Equivalent load profiles with uncertainties for MGs ($p_{Load,i} - p_{Load,i}, i = 1,2,3$)

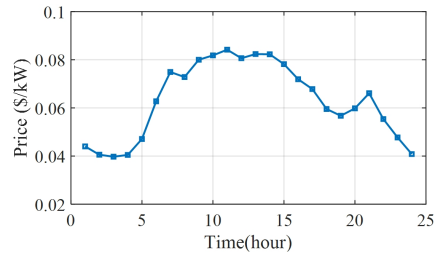

Fig. 3. The wholesale electricity prices for a day

TABLE I
System Parameters

Parameters	MG i 1	2	3
$a_{\text{DG},i}$ ($/kW/kW)	3e-5	3e-5	3e-5
$b_{\text{DG},i}$ ($/kW)	40.5e-3	40.5e-3	40.5e-3
$c_{\text{DG},i}$ ($)	0.04	0.04	0.04
$a_{\text{DG2},i}$ ($/kW/kW)	15.7e-5	19.75e-5	15.7e-5
$b_{\text{DG2},i}$ ($/kW)	35.5e-3	30.5e-3	35.5e-3
$c_{\text{DG2},i}$ ($)	0.04	0.04	0.04
$c_{\text{ESS},i}$ ($/kW)	0.01	0.01	0.01
$P_{\text{UG,max},i}$ (kW)	300	-	-
$R_{\text{DG,up},i}$,$R_{\text{DG,down},i}$ (kW/h)	80	40	40
$P_{\text{DG,max},i}$,$P_{\text{DG,min},i}$ (kW)	300,40	100,10	80,10
$R_{\text{DG2,up},i}$,$R_{\text{DG2,down},i}$ (kW/h)	80	40	40
$P_{\text{DG2,max},i}$,$P_{\text{DG2,min},i}$ (kW)	0,0	50,0	50,0
$P_{\text{ESS,max},i}$ (kW)	50	50	50
$E_{\text{ESS,min},i}$ (kWh)	50	50	80
$P_{\text{MG,max},i}$ (kW)	50	50	50
$\eta_{\text{ESS,c},i}$,$\eta_{\text{ESS,dc},i}$	0.95	0.95	0.95

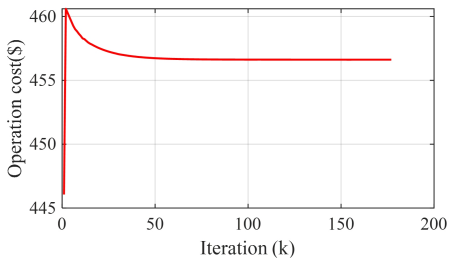

Fig. 4. Convergence curve of total operational costs

Fig. 5 presents the scheduling results of each MG in the cluster including the optimal power set points for power outputs of UG, DGs, ESSs and power exchange among MGs. As can be observed, all the units operate within their operating constraints. During t=8h-20h, the total power generation of

This article has been accepted for publication in a future issue of this journal, but has not been fully edited. Content may change prior to final publication. Citation information: DOI 10.1109/TSTE.2020.2991096, IEEE Transactions on Sustainable Energy

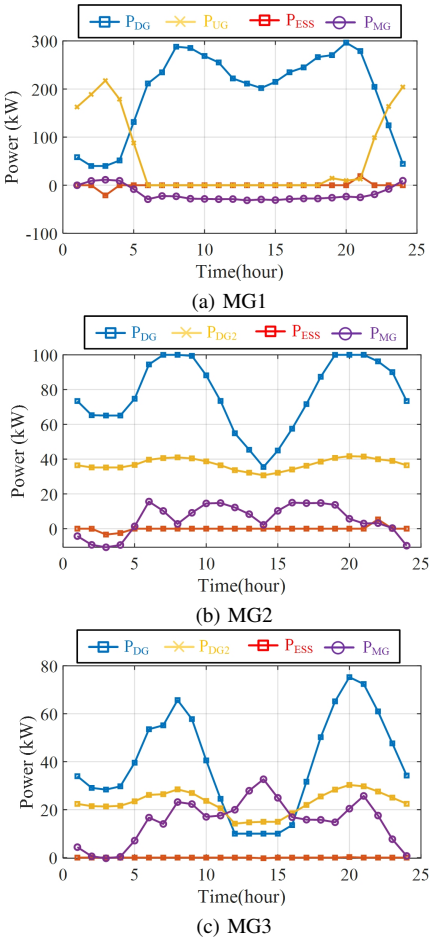

Fig. 5. Scheduling results under the proposed scheme.

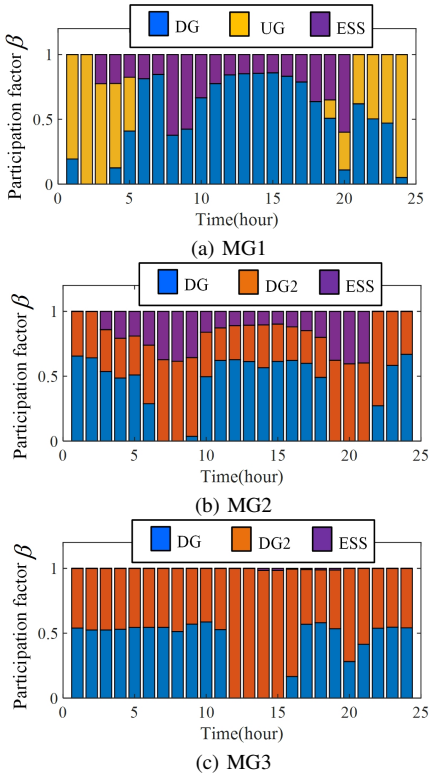

Fig. 6. Participation factor results under the proposed scheme.

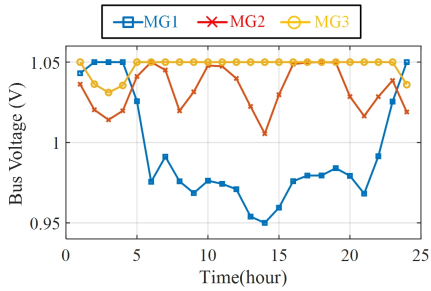

Fig. 7. Bus Voltage results of MGs

the dispatchable units reduces a lot, which is consistent with the imbalanced power profile in Fig. 2. In MG1, UG does not provide any power and participate in uncertain power sharing during t=6-18h, this is because the price of UG power at that time is higher than the incremental cost of DG. Similarly, the power sharing between DGs in MG2 and MG3 are based on their corresponding cost functions. From t=5-24h, MG2 and MG3 transfer power to MG1 because DG in MG1 is higher than DGs in MG2 and MG3 even with the tranmission loss; then the overall economy of the cluster is improved. Therefore, optimal power scheduling is achieved and the power sharing among the MGs can improve the system economy and efficiency.

The participation factor results for each MG in the cluster is shown in Fig. 6. When power dispatch of UG and DGs are zero (UG in MG1 at t=6-18h) or reaching their maximum limitation (DG1 in MG2 at t=7-9, 19-21h and DG1 in MG3 at 12-15h, as shown in Fig. 5), their participation factors in Fig. 6 are also zero, i.e. they do not participate in uncertain power sharing. When capacities are sufficient for dispatchable units, the participation factors are determined by their cost functions. Therefore, the participation of each unit in sharing of uncertain power variation is determined by the corresponding power capacity left after the scheduling and their cost functions. Moreover, the participation factors in individual MGs always sum to be the unity value, which means that the power fluctuations of PV and loads are compensated by the UG, DG and ESS locally within an individual MG; thus the amount of energy exchanged between interconnected MGs becomes a controllable value, which could aid for energy trading in the future electricity market. This local uncertainty management also helps to manage the optimization of the overall system in a distributed manner with the information privacy of each MG entity.

Bus voltage results of MGs are shown in Fig. 7. It reveals that the voltages are within the allowable range (-5% - 5%).

The results of participation factors are converted to the corresponding droop coefficient values based on (26)-(29) for real-time controllers. Table II shows the droop coefficient values for MG2 as a demonstration example.

Fig. 8 shows the simulation results in Matlab/Simulink when the local controller responds to the scheduling results from operation level of MG2 at 9h, 10h and 11h (which is 10s, 20s and 30s in the simulation results). It reveals that real-time values follow the scheduling results well if no uncertainties are considered; the system stably transits to another operating

This article has been accepted for publication in a future issue of this journal, but has not been fully edited. Content may change prior to final publication. Citation information: DOI 10.1109/TSTE.2020.2991096, IEEE Transactions on Sustainable Energy

TABLE II
OPTIMAL DROOP COEFFICIENTS FOR MG2

Time (h)	1	2	3	4	5	6
$m_{DG,2}$(V/kW)	0.100	0.100	0.053	0.086	0.075	0.100
$m_{DG2,2}$(V/kW)	0.191	0.180	0.087	0.136	0.127	0.064
$m_{ESS,2}$(V/kW)	10	10	0.200	0.200	0.200	0.110
Time (h)	7	8	9	10	11	12
$m_{DG,2}$(V/kW)	10	10	10	0.065	0.041	0.035
$m_{DG2,2}$(V/kW)	0.119	0.125	0.118	0.094	0.101	0.084
$m_{ESS,2}$(V/kW)	0.200	0.200	0.200	0.200	0.200	0.200
Time (h)	13	14	15	16	17	18
$m_{DG,2}$(V/kW)	0.035	0.037	0.032	0.039	0.050	0.082
$m_{DG2,2}$(V/kW)	0.076	0.063	0.068	0.093	0.118	0.129
$m_{ESS,2}$(V/kW)	0.200	0.200	0.200	0.200	0.200	0.200
Time (h)	19	20	21	22	23	24
$m_{DG,2}$(V/kW)	10	10	10	0.100	0.100	0.099
$m_{DG2,2}$(V/kW)	0.121	0.136	0.132	0.037	0.140	0.200
$m_{ESS,2}$(V/kW)	0.200	0.200	0.200	10	10	10

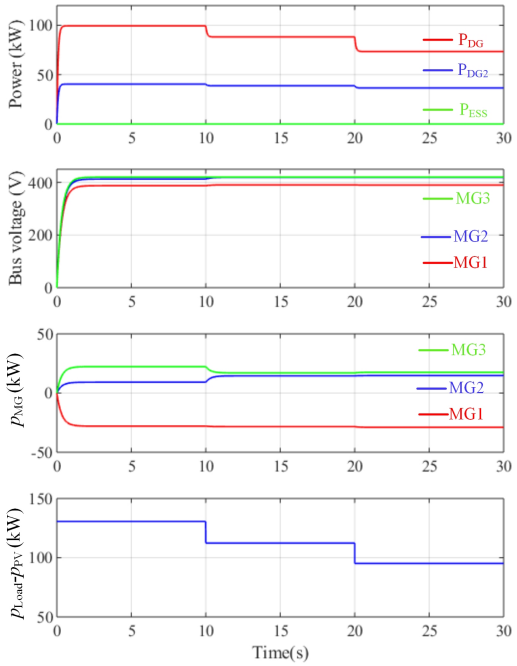

Fig. 8. Simulation results when local controller responds to the scheduling results from operation level of MG2 at 9h, 10h and 11h (which is at 10s, 20s and 30s in the simulation)

point when local controllers receive new optimal scheduling results from the operation layer.

Fig. 9 presents the dynamic results of power output of DG, DG2 and ESS as well as the bus voltage in MG2 and power output of MG2 during 9h-10h with the fluctuations of PV and load in Matlab/Simulink. As can be observed, power sharing of each dispatchable unit is around its optimal power set point (as illustrated in Fig. 5(b)) and the sharing of the fluctuation is based on the corresponding participation factor (as presented in Fig. 6 (b)). The bus voltage is regulated within the required operating limit and power exchange of MG2 with the cluster network is controlled at the scheduled value (14.54kW). It reveals that the control implementation works effectively.

To evaluate the results with different uncertainty levels, operational costs results with regard to different maximum

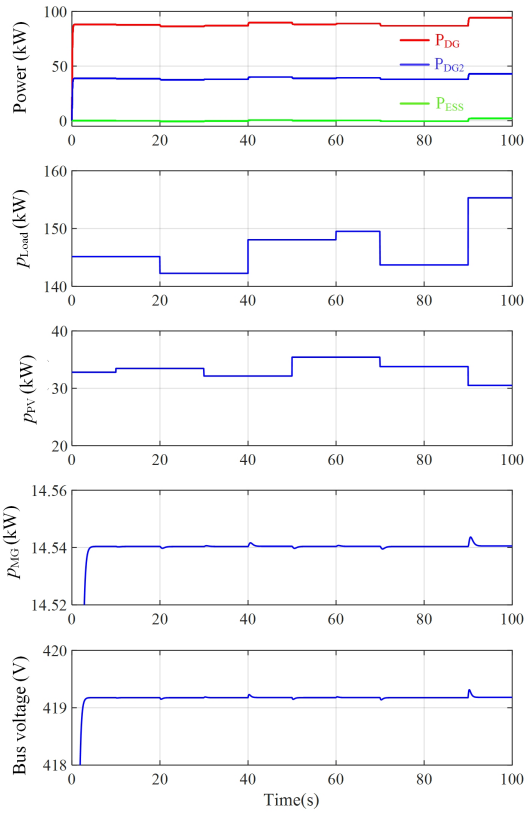

Fig. 9. Simulation results of MG2 during 9h-10h with PV and load fluctuations in Matlab/Simulink

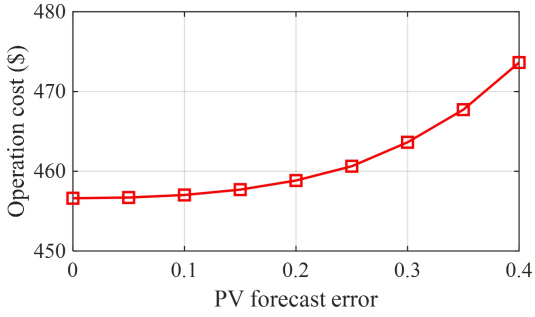

Fig. 10. Operational costs under different uncertainty levels of PV forecasting

forecasting errors of PV $\xi_{\mathrm{PV},i}^{\max}$ are investigated, as shown in Fig. 10. It shows that, when the boundary of PV forecasting error $\xi_{\mathrm{PV},i}^{\max}$ increases from 0 to 0.4 (i.e., the uncertainty boundary $\xi_i^{\max}$ is 0.1 to 0.5), the operating cost increases; higher uncertainty levels (i.e., higher robustness) will lead to higher operating costs (i.e., more conservative results). This result is consistent with the trade-off between the solution robustness and economy.

To show the scalability of the proposed algorithm, a system with 30 MGs interconnected through a modified IEEE 123-bus test system is simulated. Fig. 11 shows the convergence of the operating cost of the large-scale system. The corresponding optimal operating cost is 3123$ with 21 iterations. The corresponding time to calculate an update of the control variable is 63.4186s for the 30-MG system. The calculation time of an update can be shorter with a highspeed CPU. Compared with

This article has been accepted for publication in a future issue of this journal, but has not been fully edited. Content may change prior to final publication. Citation information: DOI 10.1109/TSTE.2020.2991096, IEEE Transactions on Sustainable Energy

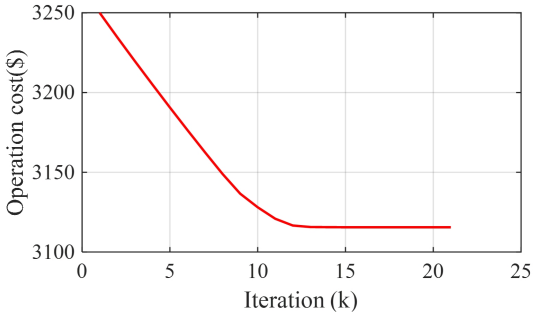

Fig. 11. Convergence of the total operating cost for a 30-microgrid system

TABLE III
SYSTEM PARAMETERS AND CONTROL PARAMETERS FOR STABILITY ANALYSIS OF MG2

Variables	Description	Value
E	Converter input voltage	100V
L	Inductor	2mH
C	Capacitor	1mF
k_{vp}, k_{vi}	voltage loop PI gains	1,50
k_{ip}, k_{ii}	Current loop PI gains	1,150
P_{CPL}	constant power load	30kW
V_{ref}	Reference voltage	400V

the calculation time of 25.5s for the 3-MG system in Fig. 4, even though the computing time increases with a large-scale system, the update time is still short compared with one scheduling interval.

The change of droop gain in the real-time controller will cause the change of the power sharing in different distributed generators (DGs), as shown in Fig. 8. As the control bandwidth of droop controller is much larger than the inner voltage+current controller of the DG interface converter, the output of the droop controller can be seen as a steady state value and can be quickly tracked by the inner controller. Therefore, the update of the droop gain will not cause unstable as long as the droop gains selected do not violate system small signal stability. To ensure the optimized droop gains always satisfy the stability requirement, a small signal stability analysis is performed. Here MG 2 with two DGs and one ESS is investigated. The DGs are connected by DC/DC boost converters and the ESS is connected by bidirectional DC/DC boost converters. As the resistive load has damping effect and the worst case in terms of stability in DC microgrid is the pure constant power load case, the load is assumed to be pure constant power load. The small signal model of the system can be built based on [32]. The system parameters are listed in Table III. Fig. 12 investigates the eigenvalue loci of the system with all the droop gains vary from 0.01 to 0.2 with a step increase of 0.01 (V/kW). It shows that all the eigenvalues are on the left half plane and thus the system is always stable.

VI. CONCLUSION

This paper proposes a hierarchically coordinated operation and control scheme for DC MG clusters. The operation layer optimizes the scheduling power set points and droop curves simultaneously to minimize the total operating cost with the consideration of the real-time local controller's response

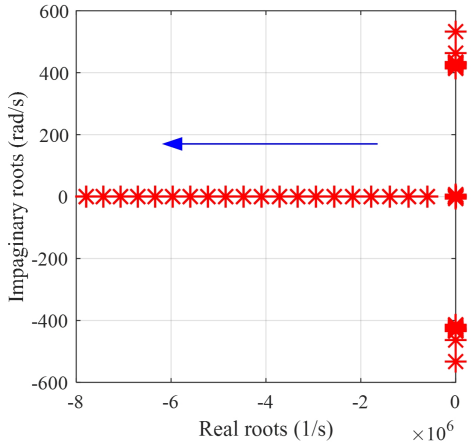

Fig. 12. The eigenvalue loci of the system with all the droop gains vary from 0.01 to 0.2 with a step increase of 0.01 (V/kW).

against uncertain fluctuations in real time; in the real-time control layer, the real-time droop controllers respond to the real-time power fluctuations through the optimal droop curves near the optimal power set points. The coordinated optimization problem is formed as an affinely adjustable robust optimization model and solved by by ADMM. The practical implementation of the proposed scheme is demonstrated in Matlab to verify the effectiveness of the proposed scheme. It is shown that proposed approach achieves decentralized power sharing at the real-time control layer and distributed optimization at operation layer, thus it features high scalability and reliability, especially for a MG cluster with open-boundary and plug-and-play characteristics.

APPENDIX

The formulation of the robust counterparts of (5)-(12) is presented below:

By substituting the affine policies (22)-(25) into (5)-(12), we have:

$$0 \le P_{\text{UG},i} + \beta_{\text{UG},i}\xi_i \le P_{\text{UG,max},i}, \forall t \in \mathcal{T} \tag{A.1}$$

$$P_{\text{DG,min},i} \le P_{\text{DG},i} + \beta_{\text{DG},i}\xi_i \le P_{\text{DG,max},i}, \forall t \in \mathcal{T} \tag{A.2}$$

$$\begin{aligned} P_{\text{DG},i} - R_{\text{DG,down},i} \le P_{\text{DG},i} + \beta_{\text{DG},i}\xi_i \\ \le P_{\text{DG},i} + R_{\text{DG,up},i}, \forall t \in \mathcal{T} \end{aligned} \tag{A.3}$$

$$0 \le P_{\text{ESS,dc},i} - P_{\text{ESS,c},i} + \beta_{\text{ESS},i}\xi_i \le P_{\text{ESS,dc,max},i}, \forall t \in \mathcal{T} \tag{A.4}$$

$$0 \le -P_{\text{ESS,dc},i} + P_{\text{ESS,c},i} - \beta_{\text{ESS},i}\xi_i \le P_{\text{ESS,c,max},i}, \forall t \in \mathcal{T} \tag{A.5}$$

$$E_{\text{ESS,min},i} \le E_{\text{ESS},i}(t) + \beta_{\text{ESS},i}\xi_i \Delta t \le E_{\text{ESS,max},i}, \forall t \in \mathcal{T} \tag{A.6}$$

Considering $\xi_i \in [-\xi_i^{\max}, \xi_i^{\max}]$ in (21), then the robust counterparts of (5)-(12) are formulated as

$$\begin{aligned} \beta_{\text{UG},i}(t)\xi_i^{\max} \le P_{\text{UG},i}(t) \\ \le P_{\text{UG,max},i} - \beta_{\text{UG},i}(t)\xi_i^{\max}, \forall t \in \mathcal{T} \end{aligned} \tag{A.7}$$

$$\begin{aligned} P_{\text{DG,min},i} + \beta_{\text{DG},i}(t)\xi_i^{\max} \le P_{\text{DG},i}(t) \\ \le P_{\text{DG,max},i} - \beta_{\text{DG},i}(t)\xi_i^{\max}, \forall t \in \mathcal{T} \end{aligned} \tag{A.8}$$

$$P_{\mathrm{DG},i}(t) - R_{\mathrm{DG,down},i} + \beta_{\mathrm{DG},i}(t)\xi_i^{\max} \le P_{\mathrm{DG},i}(t) \le P_{\mathrm{DG},i}(t) + R_{\mathrm{DG,up},i} - \beta_{\mathrm{DG},i}(t)\xi_i^{\max}, \forall t \in \mathcal{T} \quad \text{(A.9)}$$

$$-P_{\mathrm{ESS,c,max},i} + \beta_{\mathrm{ESS},i}(t)\xi_i^{\max} \le P_{\mathrm{ESS,dc},i}(t) - P_{\mathrm{ESS,c},i}(t) \le P_{\mathrm{ESS,dc,max},i} - \beta_{\mathrm{ESS},i}(t)\xi_i^{\max}, \forall t \in \mathcal{T} \quad \text{(A.10)}$$

$$E_{\mathrm{ESS,min},i} + \beta_{\mathrm{ESS},i}(t)\xi_i^{\max}\Delta t \le E_{\mathrm{ESS},i}(t) \le E_{\mathrm{ESS,max},i} - \beta_{\mathrm{ESS},i}(t)\xi_i^{\max}\Delta t, \forall t \in \mathcal{T} \quad \text{(A.11)}$$

where power set point values $\mathbf{P}_i(t) := \{P_{\mathrm{UG},i}(t), P_{\mathrm{DG},i}(t), P_{\mathrm{ESS,c},i}(t), P_{\mathrm{ESS,dc},i}(t), P_{\mathrm{MG},i}(t)\}$, $t \in \mathcal{T}$ and participation factors $\beta_i(t) := \{\beta_{\mathrm{UG},i}(t), \beta_{\mathrm{DG},i}(t), \beta_{\mathrm{ESS},i}(t)\}, t \in \mathcal{T}$ are decision variables to be optimized.

REFERENCES

[1] S. Parhizi, H. Lotfi, A. Khodaei, and S. Bahramirad, "State of the art in research on microgrids: A review," *IEEE Access*, vol. 3, pp. 890–925, 2015.

[2] J. Rocabert, A. Luna, F. Blaabjerg, and P. Rodríguez, "Control of power converters in AC microgrids," *IEEE Transactions on Power Electronics*, vol. 27, no. 11, pp. 4734–4749, Nov. 2012.

[3] D. E. Olivares, A. Mehrizi-Sani, A. H. Etemadi, C. A. Cañizares, R. Iravani, M. Kazerani, A. H. Hajimiragha, O. Gomis-Bellmunt, M. Saeedifard, R. Palma-Behnke, G. A. Jiménez-Estévez, and N. D. Hatziargyriou, "Trends in microgrid control," *IEEE Transactions on Smart Grid*, vol. 5, no. 4, pp. 1905–1919, Jul. 2014.

[4] J. Xiao, P. Wang, L. Setyawan, and Q. Xu, "Multi-level energy management system for real-time scheduling of DC microgrids with multiple slack terminals," *IEEE Transactions on Energy Conversion*, vol. 31, no. 1, pp. 392–400, Mar. 2016.

[5] T. Dragičević, X. Lu, J. C. Vasquez, and J. M. Guerrero, "DC microgrids—part i: A review of control strategies and stabilization techniques," *IEEE Transactions on Power Electronics*, vol. 31, no. 7, pp. 4876–4891, Jul. 2016.

[6] L. Meng, Q. Shafiee, G. F. Trecate, H. Karimi, D. Fulwani, X. Lu, and J. M. Guerrero, "Review on control of DC microgrids and multiple microgrid clusters," *IEEE Journal of Emerging and Selected Topics in Power Electronics*, vol. 5, no. 3, pp. 928–948, Sep. 2017.

[7] S. Moayedi and A. Davoudi, "Distributed tertiary control of DC microgrid clusters," *IEEE Transactions on Power Electronics*, vol. 31, no. 2, pp. 1717–1733, Feb. 2016.

[8] J. M. Guerrero, J. C. Vasquez, J. Matas, L. G. de Vicuna, and M. Castilla, "Hierarchical control of droop-controlled AC and DC microgrids—a general approach toward standardization," *IEEE Transactions on Industrial Electronics*, vol. 58, no. 1, pp. 158–172, Jan. 2011.

[9] C. Jin, P. Wang, J. Xiao, Y. Tang, and F. H. Choo, "Implementation of hierarchical control in DC microgrids," *IEEE Transactions on Industrial Electronics*, vol. 61, no. 8, pp. 4032–4042, Aug. 2014.

[10] Q. Xu, X. Hu, P. Wang, J. Xiao, P. Tu, C. Wen, and M. Y. Lee, "A decentralized dynamic power sharing strategy for hybrid energy storage system in autonomous dc microgrid," *IEEE Transactions on Industrial Electronics*, vol. 64, no. 7, pp. 5930–5941, July 2017.

[11] I. U. Nutkani, P. C. Loh, P. Wang, and F. Blaabjerg, "Cost-prioritized droop schemes for autonomous AC microgrids," *IEEE Transactions on Power Electronics*, vol. 30, no. 2, pp. 1109–1119, Feb. 2015.

[12] Q. Xu, J. Xiao, P. Wang, and C. Wen, "A decentralized control strategy for economic operation of autonomous AC, DC, and hybrid AC/DC microgrids," *IEEE Transactions on Energy Conversion*, vol. 32, no. 4, pp. 1345–1355, Dec. 2017.

[13] S. Sahoo and S. Mishra, "A multi-objective adaptive control framework in autonomous DC microgrid," *IEEE Transactions on Smart Grid*, vol. 9, no. 5, pp. 4918–4929, Sep. 2018.

[14] S. Moayedi and A. Davoudi, "Unifying distributed dynamic optimization and control of islanded DC microgrids," *IEEE Transactions on Power Electronics*, vol. 32, no. 3, pp. 2329–2346, Mar. 2017.

[15] P. Tian, X. Xiao, K. Wang, and R. Ding, "A hierarchical energy management system based on hierarchical optimization for microgrid community economic operation," *IEEE Transactions on Smart Grid*, vol. 7, no. 5, pp. 2230–2241, 2016.

[16] A. Gholami and X. A. Sun, "Towards resilient operation of multi-microgrids: An misocp-based frequency-constrained approach," *IEEE Transactions on Control of Network Systems*, vol. 6, no. 3, pp. 925–936, 2018.

[17] Z. Wang, B. Chen, J. Wang, M. M. Begovic, and C. Chen, "Coordinated energy management of networked microgrids in distribution systems," *IEEE Transactions on Smart Grid*, vol. 6, no. 1, pp. 45–53, 2014.

[18] Y. Liu, Y. Li, H. B. Gooi, Y. Jian, H. Xin, X. Jiang, and J. Pan, "Distributed robust energy management of a multimicrogrid system in the real-time energy market," *IEEE Transactions on Sustainable Energy*, vol. 10, no. 1, pp. 396–406, 2017.

[19] Q. Zhang, K. Dehghanpour, Z. Wang, and Q. Huang, "A learning-based power management method for networked microgrids under incomplete information," *IEEE Transactions on Smart Grid*, 2019.

[20] Y. Du and F. Li, "Intelligent multi-microgrid energy management based on deep neural network and model-free reinforcement learning," *IEEE Transactions on Smart Grid*, 2019.

[21] W. Su, J. Wang, and J. Roh, "Stochastic energy scheduling in microgrids with intermittent renewable energy resources," *IEEE Transactions on Smart Grid*, vol. 5, no. 4, pp. 1876–1883, Jul. 2014.

[22] T. Zhao, X. Pan, S. Yao, C. Ju, and L. Li, "Strategic bidding of hybrid ac/dc microgrid embedded energy hubs: A two-stage chance constrained stochastic programming approach," *IEEE Transactions on Sustainable Energy*, 2018.

[23] W. Chen, X. Ruan, H. Yan, and K. T. Chi, "Dc/dc conversion systems consisting of multiple converter modules: stability, control, and experimental verifications," *IEEE Transactions on Power Electronics*, vol. 24, no. 6, pp. 1463–1474, 2009.

[24] C. Wan, Z. Xu, P. Pinson, Z. Y. Dong, and K. P. Wong, "Probabilistic forecasting of wind power generation using extreme learning machine," *IEEE Transactions on Power Systems*, vol. 29, no. 3, pp. 1033–1044, 2013.

[25] R. A. Jabr, "Adjustable robust opf with renewable energy sources," *IEEE Transactions on Power Systems*, vol. 28, no. 4, pp. 4742–4751, Nov. 2013.

[26] Y. An and B. Zeng, "Exploring the modeling capacity of two-stage robust optimization: Variants of robust unit commitment model," *IEEE transactions on Power Systems*, vol. 30, no. 1, pp. 109–122, 2014.

[27] C. Zhang, Y. Xu, Z. Y. Dong, and J. Ma, "Robust operation of microgrids via two-stage coordinated energy storage and direct load control," *IEEE Transactions on Power Systems*, vol. 32, no. 4, pp. 2858–2868, 2016.

[28] Q. Li and V. Vittal, "Convex hull of the quadratic branch ac power flow equations and its application in radial distribution networks," *IEEE Transactions on Power Systems*, vol. 33, no. 1, pp. 839–850, 2017.

[29] S. Boyd, N. Parikh, E. Chu, B. Peleato, and J. Eckstein, "Distributed optimization and statistical learning via the alternating direction method of multipliers," *Foundations and Trends® in Machine Learning*, vol. 3, no. 1, pp. 1–122, 2011.

[30] T. Zhao, J. Chen, Qifang Zhang, and L. Yu, "Energy/reserve sharing dispatch for interconnected multiple microgrids based on adaptive robust optimization," *Power System Technology*, vol. 40, no. 12, pp. 3783–3789, 2016.

[31] D. W. Van der Meer, J. Widén, and J. Munkhammar, "Review on probabilistic forecasting of photovoltaic power production and electricity consumption," *Renewable and Sustainable Energy Reviews*, vol. 81, pp. 1484–1512, 2018.

[32] Q. Xu, P. Wang, J. Xiao, C. Wen, and L. M. Yeong, "Modeling and stability analysis of hybrid energy storage system under hierarchical control," in *Proc. IEEE PES Asia-Pacific Power and Energy Engineering Conf. (APPEEC)*, Nov. 2015, pp. 1–5.

Qianwen Xu (S'14-M'18) received the B.Sc. degree from Tianjin University, China in 2014 and PhD degree from Nanyang Technological University, Singapore in 2018, both in electrical engineering. She has worked as a research associate in Hong Kong Polytechnic University, Hong Kong, and a postdoc research fellow in Aalborg University, Denmark, in 2018. Currently, she is a Wallenberg-NTU Presidential Postdoc Fellow in Nanyang Technological University, Singapore. Her research interests include control, stability, reliability and optimization of microgrids and smart grids.

Yan Xu (S'10-M'13-SM'19) received the B.E. and M.E degrees from South China University of Technology, Guangzhou, China in 2008 and 2011, respectively, and the Ph.D. degree from The University of Newcastle, Australia, in 2013. He is now the Nanyang Assistant Professor at School of Electrical and Electronic Engineering, Nanyang Technological University (NTU), and a Cluster Director at Energy Research Institute @ NTU (ERI@N), Singapore. Previously, he held The University of Sydney Postdoctoral Fellowship in Australia. His research interests include power system stability and control, microgrid, and data-analytics for smart grid applications. Dr Xu is an Editor for IEEE TRANSACTIONS ON SMART GRID, IEEE POWER ENGINEERING LETTERS, CSEE Journal of Power and Energy Systems, and an Associate Editor for IET Generation, Transmission & Distribution.

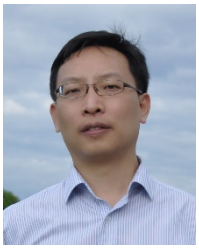

Z hao Xu (M'06-SM'12) received B.Eng, M.Eng and Ph.D degree from Zhejiang University, National University of Singapore, and The University of Queensland in 1996, 2002 and 2006, respectively. From 2006 to 2009, he was an Assistant and later Associate Professor with the Centre for Electric Technology, Technical University of Denmark, Lyngby, Denmark. Since 2010, he has been with The Hong Kong Polytechnic University, where he is currently a Professor in the Department of Electrical Engineering and Leader of Smart Grid Research Area (http://www.mypolyuweb.hk/eezhaoxu/). He is also a foreign Associate Staff of Centre for Electric Technology, Technical University of Denmark. His research interests include demand side, grid integration of wind and solar power, electricity market planning and management, and AI applications. He is an Editor of the Electric Power Components and Systems, the IEEE PES Power Engineering Letter, and the IEEE Transactions on Smart Grid. He is currently the Chairman of IEEE PES/IES/PELS/IAS Joint Chapter in Hong Kong Section.

Lihua Xie received the Ph.D. degree in electrical engineering from the University of Newcastle, Australia, in 1992. Since 1992, he has been with the School of Electrical and Electronic Engineering, Nanyang Technological University, Singapore, where he is currently a professor and Director, Delta-NTU Corporate Laboratory for Cyber-Physical Systems. He served as the Head of Division of Control and Instrumentation from July 2011 to June 2014. He held teaching appointments in the Department of Automatic Control, Nanjing University of Science and Technology from 1986 to 1989.

Dr Xie's research interests include robust control and estimation, networked control systems, multi-agent networks, localization and unmanned systems. He is an Editor-in-Chief for Unmanned Systems and an Associate Editor for IEEE Transactions on Network Control Systems. He has served as an editor of IET Book Series in Control and an Associate Editor of a number of journals including IEEE Transactions on Automatic Control, Automatica, IEEE Transactions on Control Systems Technology, and IEEE Transactions on Circuits and Systems-II. He was an IEEE Distinguished Lecturer (Jan 2012 – Dec 2014) and an elected member of Board of Governors, IEEE Control System Society (Jan 2016-Dec 2018). Dr Xie is Fellow of IEEE, Fellow of IFAC and Fellow of Chinese Automation Association.

Frede Blaabjerg (S'86–M'88–SM'97–F'03) was with ABB-Scandia, Randers, Denmark, from 1987 to 1988. From 1988 to 1992, he got the PhD degree in Electrical Engineering at Aalborg University in 1995. He became an Assistant Professor in 1992, an Associate Professor in 1996, and a Full Professor of power electronics and drives in 1998. From 2017 he became a Villum Investigator. He is honoris causa at University Politehnica Timisoara (UPT), Romania and Tallinn Technical University (TTU) in Estonia.

His current research interests include power electronics and its applications such as in wind turbines, PV systems, reliability, harmonics and adjustable speed drives. He has published more than 600 journal papers in the fields of power electronics and its applications. He is the co-author of four monographs and editor of ten books in power electronics and its applications.

He has received 31 IEEE Prize Paper Awards, the IEEE PELS Distinguished Service Award in 2009, the EPE-PEMC Council Award in 2010, the IEEE William E. Newell Power Electronics Award 2014, the Villum Kann Rasmussen Research Award 2014 and the Global Energy Prize in 2019. He was the Editor-in-Chief of the IEEE TRANSACTIONS ON POWER ELECTRONICS from 2006 to 2012. He has been Distinguished Lecturer for the IEEE Power Electronics Society from 2005 to 2007 and for the IEEE Industry Applications Society from 2010 to 2011 as well as 2017 to 2018. In 2019-2020 he serves a President of IEEE Power Electronics Society. He is Vice-President of the Danish Academy of Technical Sciences too. He is nominated in 2014-2018 by Thomson Reuters to be between the most 250 cited researchers in Engineering in the world.